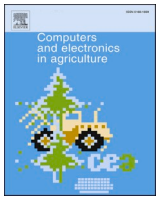
Computers and Electronics in Agriculture 213 (2023) 108225



Contents lists available at ScienceDirect

Computers and Electronics in Agriculture

journal homepage: www.elsevier.com/locate/compag





Fruit detachment force of multiple varieties kiwifruit with different fruit-stem angles for designing universal robotic picking end-effector

Wentai Fang [a], Zhenchao Wu [a], Weiwu Li [a], Xiaoming Sun [a], Wulan Mao [a,e], Rui Li [a,d], Yaqoob Majeed [f], Longsheng Fu [a,b,c,d,*]

[a] College of Mechanical and Electronic Engineering, Northwest A&F University, Yangling, Shaanxi, 712100, China
[b] Key Laboratory of Agricultural Internet of Things, Ministry of Agriculture and Rural Affairs, Yangling, Shaanxi 712100, China
[c] Shaanxi Key Laboratory of Agricultural Information Perception and Intelligent Service, Yangling, Shaanxi 712100, China
[d] Northwest A&F University Shenzhen Research Institute, Shenzhen, Guangdong 518000, China
[e] Institute of Agricultural Mechanization, Xinjiang Academy of Agricultural Sciences, Urumqi 830000, China
[f] Faculty of Agricultural Engineering and Technology, University of Agriculture, Faisalabad 38000, Pakistan

ARTICLE INFO

Keywords:
Multiple varieties kiwifruit
Fruit holding device
Fruit detachment force
Fruit-stem angles
Picking robot

ABSTRACT

Fruit detachment force (FDF) between fruit and stem, is one of the important physical parameters for designing fruit picking robot. Orchards planted with multiple varieties kiwifruit generally exist in China because of their rich variety resources. FDFs at different fruit-stem angles (FSA) for multiple varieties kiwifruit make it difficult for the fruit picking robot to maintain optimal working conditions for different varieties. Determining the FDF of a single variety is not suitable for developing a universal end-effector that enables fruit picking of multiple varieties kiwifruit. Therefore, it is necessary to measure the FDF of multiple varieties kiwifruit at different FSA. In this study, a special fixture was developed based on external characteristics of fruit, which was installed on the texture analyzer to form a platform for measuring the FDF with different FSA. Fruits of different variety with stems hand-picked, i.e. 'Hayward', 'Xuxiang', 'Huayou', 'Cuixiang' and 'Qinmei', were measured for FDF at FSAs of 180°, 160°, 140°, 120°, 100°, 80°, and 60°. Computer-controlled texture analyzer led screw drives the lifting bracket to rise for realizing the detachment of the stem and fruit. FSAs corresponding to the minimum FDF of both 'Qinmei' and 'Cuixiang' were 80°, while those of other three varieties were 60°. The FDF at the FSA of 180° was smaller compared of the FSA of 160° for 'Hayward' and 'Cuixiang'. Additionally, the stem breakage occurred when the FDF of 'Xuxiang' was measured at the FSAs of 180° or 160°. These results have potential to provide guidance for designing a universal robotic picking end-effector for multiple varieties kiwifruit.

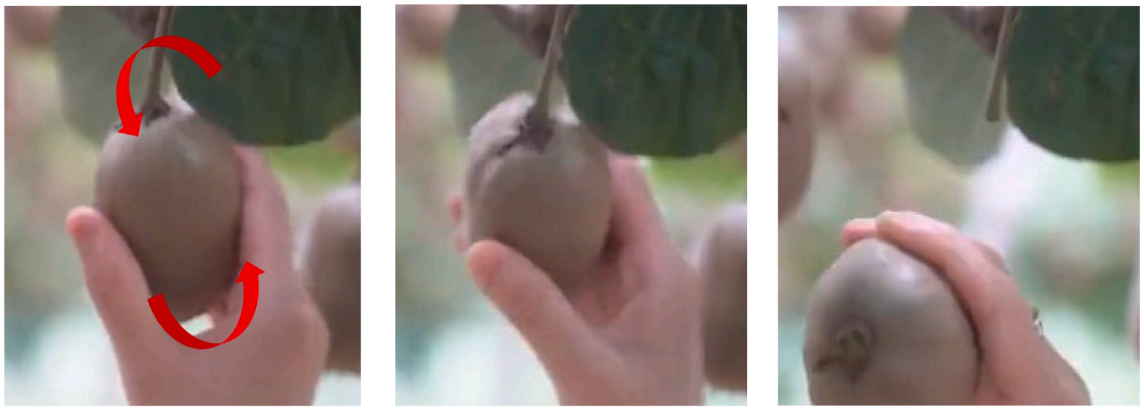
1. Introduction

Kiwifruit is a highly economical fruit and still mainly picked manually at a high cost, which is desirable for mechanical harvesting. According to the Food and Agriculture Organization of the United Nations (FAO), globally kiwifruit was planted on 2.86 million ha area with total production of 4.47 million tons in 2021. The kiwifruit industry is growing rapidly and its global sales are expected to be doubled by 2025 (Au et al., 2022). Labor costs accounting approximately 33% of variable costs in kiwifruit production (Mohammadi et al., 2010). For the kiwifruit industry, harvesting time is one of the peak demand time of the year for short-term labor with high costs (Bechar & Vigneault, 2016; Feng et al., 2013; Fu et al., 2015; Jones et al., 2019; Li et al., 2016). Therefore, it is necessary to develop fruit picking robot, which has the potential to replace human to save labor cost.

Orchard planted with multiple varieties kiwifruit has brought new challenges to the development of the fruit picking robot. Over 70 species have been developed gradually all over the world through decades of domestication and constant selection from wild kiwifruit (Zhang et al., 2020). The orchard planted with multiple varieties kiwifruit generally exist due to the abundance of varieties in China (Guo et al., 2020; Zhou et al., 2023). Additionally, kiwifruit orchards with multiple varieties helps to make full use of land resources and improve fruit yield because of the diversities in growth environment and growth cycle between different kiwifruit varieties. It also helps to meet the consumers demand and prolong the sales period. However, multiple varieties kiwifruit leads

* Corresponding author.
E-mail address: fulsh@nwafu.edu.cn (L. Fu).

https://doi.org/10.1016/j.compag.2023.108225
Received 28 May 2023; Received in revised form 31 August 2023; Accepted 2 September 2023
Available online 8 September 2023
0168-1699/© 2023 Elsevier B.V. All rights reserved.



(a) (b) (c)

Fig. 1. Model of manual kiwifruit picking. **(a)** The thumb and the remaining four fingers grasp the kiwifruit, where red arrow represents the direction of pulling and pendulum actions; **(b)** Twist the fruit with the stem as a fulcrum; **(c)** Kiwifruit and stem detachment. (For interpretation of the references to colour in this figure legend, the reader is referred to the web version of this article.)

to poor adaptability for the fruit picking robot, especially end-effector, due to the different firmness and size of fruit.

The end-effector is an important mechanism of the fruit picking robot, which has been studied based on mimicking human picking actions to achieve better performance. Different designs of end-effector for kiwifruit robotic picking have been reported (Au et al., 2020; Chen et al., 2012; Graham et al., 2018; Mu et al., 2018). For example, Williams et al., (2019) designed a two-finger end-effector, which helps to grasp the kiwifruit by a two-finger end-effector (human thumb and the remaining four fingers) and then rotate the fruit at an angle to the stem to achieve picking. However, this two-finger end-effector harvest only 51% of the kiwifruit due to the constraints for low grasping force of the end-effector because excessive grasping force induce bruises on harvested fruit and results in an economic loss (Li et al., 2016). Mu et al. (2020) proposed a method in which the end-effector approaches the fruit from below, wraps and grasps the fruit with two bionic fingers then bends the fingers to separate the fruit from the stem. Therefore, a mathematical model of picking based on the physical properties of kiwifruit is crucial for the design of the end-effector.

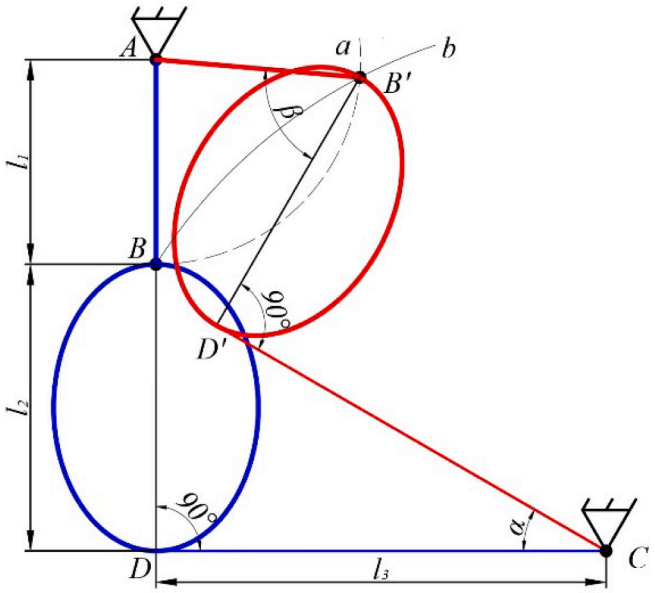


Fig. 2. Simplified model of kiwifruit picking. Point ***A*** is the link between the branch and stem; point ***B*** is the link between the fruit and stem; point ***C*** is the end-effector's hinge joint; point ***D*** is the link between the fruit and the end-effector; ***AB*** and ***CD*** represent the stem and the end-effector, respectively; ***BD*** represent the axis of inertia of the fruit; Red and blue ellipses both represent fruit; l_1, l_2, and l_3 are lengths of ***AB***, ***BD*** and ***CD***, respectively. (For interpretation of the references to colour in this figure legend, the reader is referred to the web version of this article.)

Fruit Detachment Force (FDF), detachment force between fruit and stem, is one of the important physical parameters for designing the end-effector of the fruit picking robot. Many researchers have measured the FDF for designing picking end-effectors and adjusting picking methods (Bu et al., 2021; He et al., 2017; Jiang et al., 2023; Liu et al., 2018; Parameswarakumar and Gupta, 1991; Sun et al., 2013; Yang et al., 2021). Wang et al. (2017) determined the effect of chemical treatment on FDF/Weight ratio by measuring the FDF of litchi, which improved the picking efficiency by 3.5 times compared with labor. Tekgüler et al. (2015) set picking parameters of hazelnut limbs fruit to determine the FDF/Weight and spring rate. The end-effector designed by Fu et al. (2015) obtained a picking success rate of 96% based on the significant difference in the FDF of 'Hayward' kiwifruit under different fruit-stem angle (FSA). Therefore, measuring FDFs of multiple varieties kiwifruit with different FSA is necessary for the structural design and parameter optimization of fruit-picking robots.

Texture analyzer, a high-precision device for measuring physical properties of food samples, is suitable for measuring the FDF by designing a dedicated fixture. Wang et al. (2020) calibrated a self-made hardness measurement device through a texture analyzer, which achieved a coefficient of determination of 0.9998. Perini et al. (2017) adopted a texture analyzer-based methodology to measure cell wall creep and expansin activity, which simplified the analysis of expansin. Wu et al. (2022) carried out puncture tests with the texture analyzer on 60 kiwifruits samples taken from three ripening stages and obtained hardness with an accuracy of 0.1 gf. However, there is no special fixture to fix kiwifruit for measuring the FDF.

In this study, an FDF measurement system was designed based on the geometric features of kiwifruit. A special fixture was designed based on three-dimensional (3D) kiwifruit models and was used to measure the FDF of different FSA. The main objectives of this study were: (1) to measure FDFs of multiple varieties kiwifruit; (2) to analyze the variation of the FDF of different FSA for designing a universal end-effector of kiwifruit picking robot.

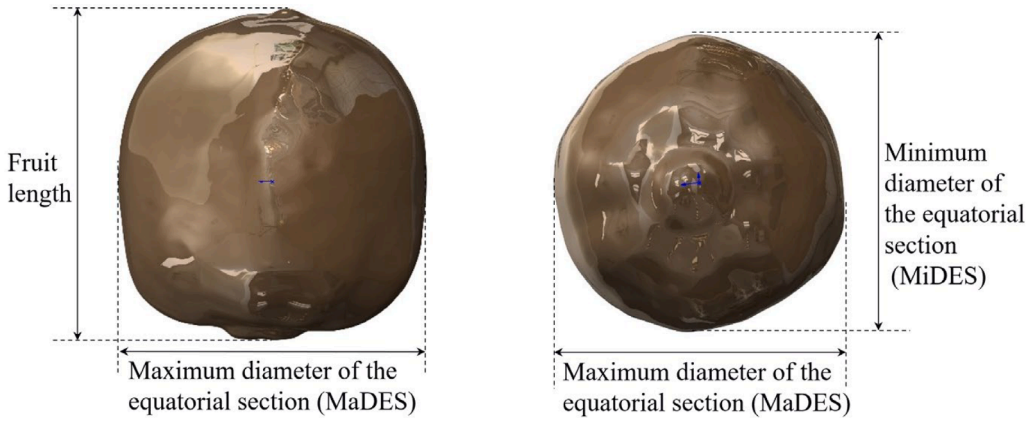


Fig. 3. The procedures of modeling kiwifruit by reverse engineering. Definitions of fruit length, maximum diameter of the equatorial section (MaDES), and minimum diameter of the equatorial section (MiDES).

2. Materials and methods

2.1. Materials

Five most widely grown kiwifruit varieties in China, i.e. 'Hayward', 'Xuxiang', 'Cuixiang', 'Qinmei', and 'Huayou', were chose for this study. These five varieties have been widely planted in the main planting areas of kiwifruits in China, which account for over 85% of the market due to their excellent fruit quality (Zhang et al., 2020). A total of 210 fruit with stems were hand-picked from orchard on October 23, 2022 in Zhouzhi, Shaanxi Province, China (34°14′ N, 108°2′ E, and 648 m in altitude). Then they were divided into five groups based on their variety for measuring the FDF at different FSA. The whole process was completed within four hours after fruit with stems were hand-picked to avoid changing the connection characteristics of fruit-stem due to water loss caused by long-term exposure to air.

2.2. Simplified model of kiwifruit picking

Manual fruit picking has been carried out by grasping the fruit with fingers and twisting the fruit in the vertical plane using the connection between the fruit and the stem. The end-effector of the fruit picking robot has often been designed with two fingers to imitate the action of manual fruit picking (one finger imitates the human thumb and the other finger imitates the other four human fingers together). As shown in Fig. 1, kiwifruit was pulled along stem axial direction by exerting tension force while also bending the stem around stem-branch joint, which involved a combination of pulling and pendulum actions. Action of manual fruit picking needs to be simplified because the end-effector is difficult to achieve the flexibility of the human hand. Hence, four assumptions are put forward in a simplified model of fruit picking, as shown in Fig. 2: (1) The connection between the stem and the branch is simplified as point ***A***; (2) The connection between the fruit and the stem is simplified as point ***B***; (3) The wrist of the end-effector is recorded as point ***C***, which is the rotating joint of the wrist of the end-effector; (4) The connection between the fruit and the end-effector is simplified as point ***D***.

The FSA was defined by establishing a simplified model for the separation process of the fruit and stem during picking. After the fruit is stably grasped by the end effector, point ***B*** will move along the dotted arc $\boldsymbol{\alpha}$ with point ***A*** as the center and the length of the fruit stem as the radius, as shown in Fig. 2. The fruit will be separated from the stem when it is moved to point ***B'***. The maximum angle of rotation of the end effector $\boldsymbol{\alpha}$ could be determined by Eq. (1). And the FSA was the maximum angle between the stem and the inertia axis of the fruit $\boldsymbol{\beta}$, which was determined by Eq. (2).

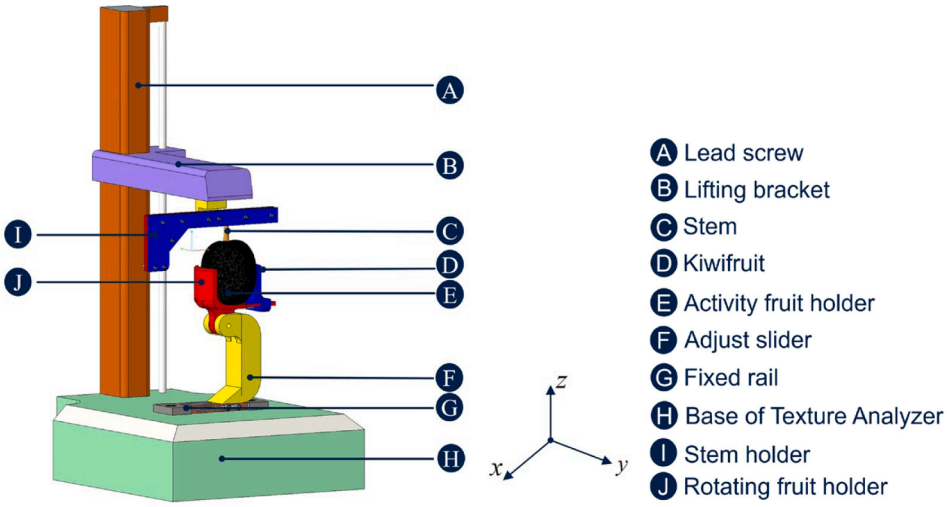


Fig. 4. Platform for measuring FDF with different FSA. The texture analyzer consisted of a lead screw, a lifting bracket, and a base of the texture analyzer. And the special fixture consisted of an activity fruit holder, an adjust slider, a stem holder, and a rotating fruit holder, which were made of PLA (Polylactic Acid) material.

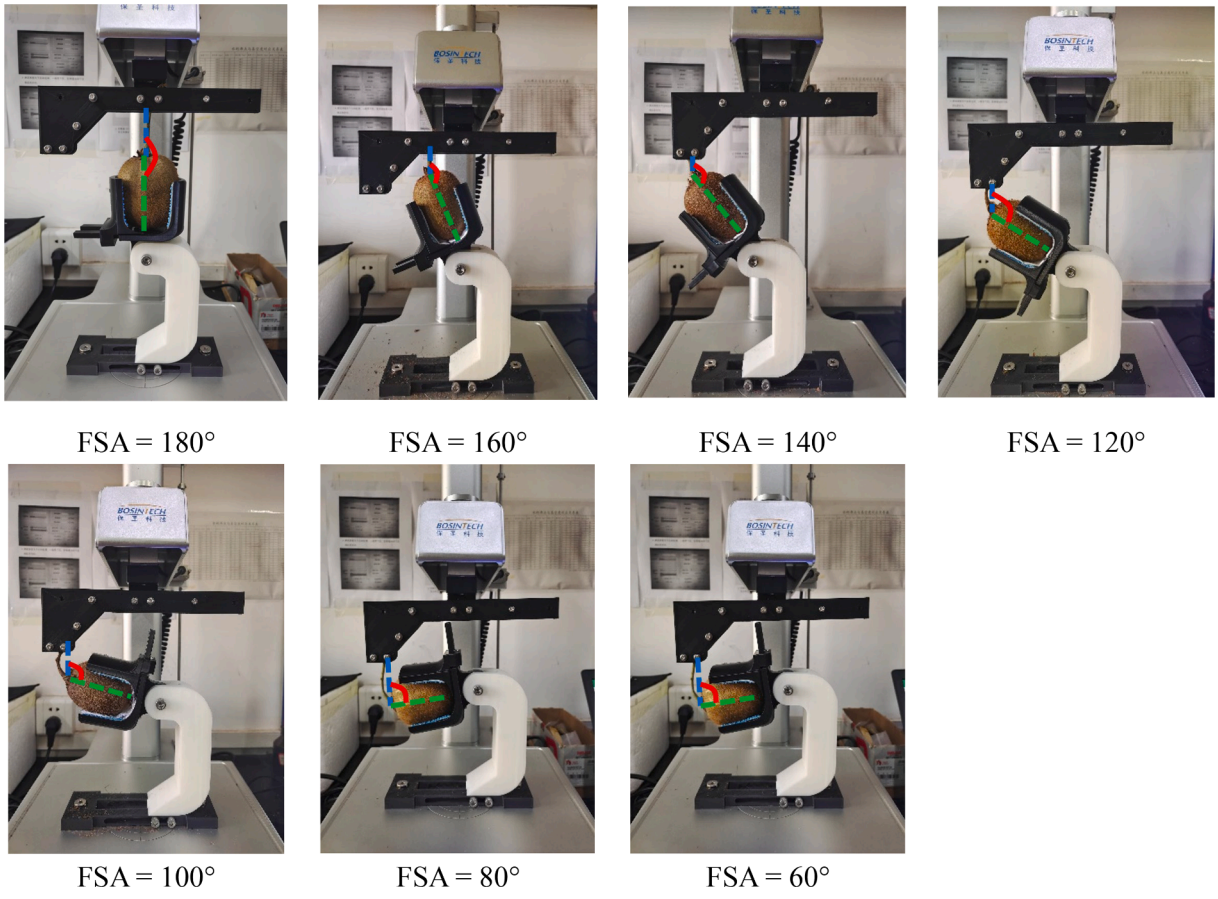


Fig. 5. FDF of kiwifruit was determined at different FSA. Angle formed by a blue dotted line and a green blue dotted line is FSA; the blue dotted line was the stem after being straightened during the FDF measurement; the green blue dotted line was the inertia axis of the fruit. (For interpretation of the references to colour in this figure legend, the reader is referred to the web version of this article.)

$$\alpha = \frac{180^{\circ}}{\pi} arctan \frac{l_1 + l_2}{l_3} - \frac{180^{\circ}}{\pi} arctan\left(tan\left(\frac{\pi}{180^{\circ}} - sec \frac{l_1 + l_2}{\sqrt{(l_1 + l_2)^2 + l_3^2}} - \frac{\pi}{180^{\circ}}\beta\right)\right) \tag{1}$$

$$\beta = \frac{180^{\circ}}{\pi}\left(\sec\left(-\frac{l_2}{\sqrt{{l_2}^2 + {l_3}^2}}\right) - \arctan\left(\frac{l_3}{l_2}\right)\right) \tag{2}$$

2.3. Experimental methods and data acquisition

2.3.1. 3D modeling of kiwifruit by reverse engineering

The premise of using the texture analyzer to measure the FDF is to design the special fixture based on external characteristics of fruit. Reverse engineering techniques were applied to accurately extract the external characteristics of fruit, which were captured by a 3D scanner (HandySCAN BLACKTM) with a measurement accuracy of 0.025 mm at the measurement speed of 1.3 million times/s. The external characteristics of a kiwifruit were obtained by scanning a kiwifruit for 30 s, which included fruit length, MaDES (Maximum diameter of the equatorial section), MiDES (Minimum diameter of the equatorial section), surface area and volume, as shown in Fig. 3. In addition, based on previous research on the FDF, the correlation of FDF with size and weight of the kiwifruit was not considered in this study (Mu et al., 2020; Fu et al., 2015).

2.3.2. Platform for measuring FDF with different FSA

The special fixture was designed and installed on the texture analyzer (TA.XTC-18, Shbosin Corp., Shanghai, China, force measurement accuracy of 0.0001 g, displacement accuracy of 0.001 mm, moving distance of test arm of 400 mm, and moving speed of 0.01 to 45.00 mm/s) to measure the FDF. It was designed based on the external characteristics of fruit measured by a 3D scanner and installed on the texture analyzer to form a platform for measuring the FDF with different FSA, as shown in Fig. 4. The stem holder was designed as a long strip of about 150 mm to ensure that the stem is still fixed after the FSA is changed. The fruit holder was adjusted by screws so as to hold the fruit easily. According to previous research on kiwifruit damage (Wu et al., 2022b; Zhang et al., 2014), a flexible and precise thread adjustment fruit holder were used to ensure that fruit compression during the separation test will not cause fruit damage. The angle of the fruit holder was changed by adjusting the adjust slider screw to alter the FSA. Computer-controlled texture analyzer led screw drives the lifting bracket to rise for realizing the detachment of the stem and fruit.

2.3.3. Determination of FDF for multiple varieties kiwifruit

In this study, the FDFs of five kiwifruit varieties were determined at seven FSAs. The texture analyzer was zeroed before determining the FDF to eliminate errors caused by the quality of the special fixture. Fu et al. (2015) proposed a detachment force experiment to measure the FDF at three FSAs of 180°, 90°, and 60°, which had a large span. Mu et al. (2020) reported a detachment force experiment to measure the FDF at five FSAs of 90°, 75°, 60°, 45°, 30°, which had a small range. Both of them were difficult to obtain detailed FDF corresponding to the FSA at a large range of small spans. Hence, 180°, 160°, 140°, 120°, 100°, 80°, and 60° were selected as the FSAs to measure the FDF. The FSA was defined as 180° when the stem is linear with the inertia axis of the fruit, and less than 180° when the stem is not linear with the inertia axis of the fruit, as

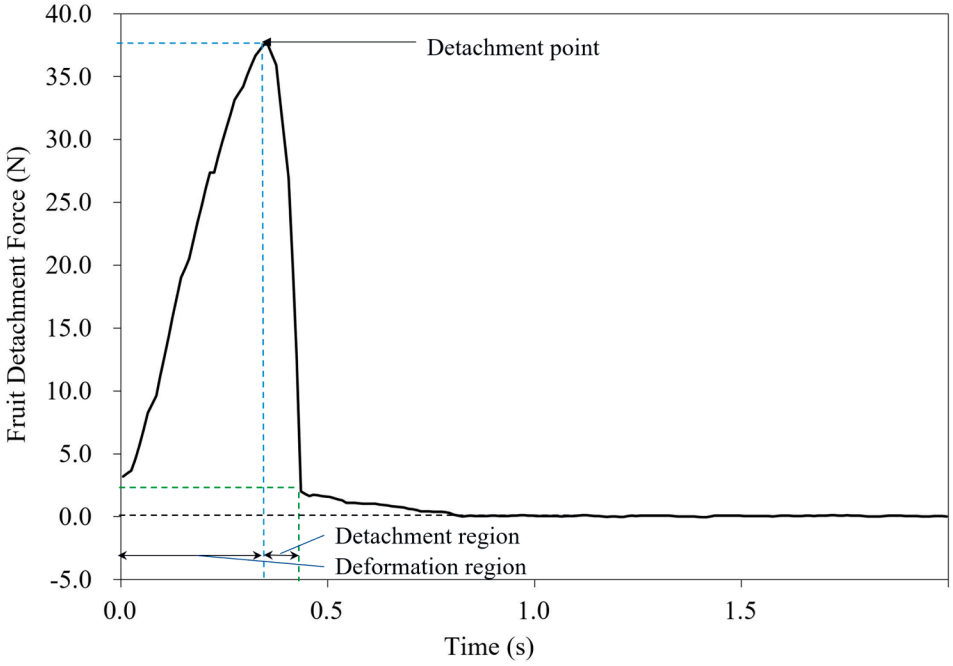


Fig. 6. Typical curve of change in tensile force corresponding to the increasing stem tensile displacement.

Table 1
Mean and standard deviation of physical properties for the five varieties kiwifruit.

Measurement	Hayward		Xuxiang		Huayou		Cuixiang		Qingmei	
	Mean	SD[a]	Mean	SD[a]	Mean	SD[a]	Mean	SD[a]	Mean	SD[a]
MaDES /mm	58.92	3.92	54.48	3.12	57.13	3.68	51.91	4.93	65.62	8.43
MiDES /mm	54.13	3.53	49.07	2.61	50.14	2.08	42.92	2.12	57.46	7.00
Fruit length (H) /mm	70.23	6.95	65.63	5.28	69.06	3.79	63.40	4.09	68.97	6.22
Mass /g	142.30	32.62	106.21	17.45	121.75	19.46	82.48	17.20	154.09	39.41
Stem length /mm	68.60	11.0	56.89	4.99	49.69	8.08	39.74	6.23	53.68	5.84

[a] SD, Standard deviation.

shown in Fig. 5. The stem holding device was raised by the texture analyzer probe at 9 mm/s to apply tension on the kiwifruit stem until the kiwifruit was detached from the stem. According to operation manual of texture analyzer (TA.XTC-18, Shbosin Corp., Shanghai, China), the maximum speed is 9 mm/s at which the texture analyzer operates to ensure measurement accuracy. For the same kiwifruit variety, FDFs of the six fruit were measured by the texture analyzer under each FSA.

The FDF increased in deformation region as the texture analyzer began to apply tension and reached maximum at detachment point, as shown in Fig. 6. As the texture analyzer continues to apply tension, the FDF decreased sharply in detachment region, where the stem gradually separates from the kiwifruit. Finally, the FDF became 0 when the stem and fruit were completely separated. The time of stem and fruit detachment is composed of the deformation region and the detachment region time.

3. Results and discussion

3.1. External characteristics of fruit

Accurate measurement of the external characteristics of the fruit provides the basis for designing more reasonable special fixture. Table 1 presents the means and standard deviations of various physical properties of 'Hayward', 'Xuxiang', 'Huayou', 'Cuixiang', and 'Qingmei' kiwifruit samples including fruit diameter, length, stem length, and mass. The fruit size and mass of different varieties vary greatly, and the average mass of 'Qinmei' is about twice that of 'Cuixiang'. The size and mass were the main parameters used for designing the fixture and the end-effector. The length of the fruit fixture is designed to be 45 mm and the length of the stem fixture is designed to be 150 mm so as not to affect the FSA measuring range. The fruit length and stem length provides the basis for designing the action parameters of the end-effector. The FSA range was determined from 180° to 60° by fruit size and stem length.

3.2. FDF of 'Hayward' kiwifruit

The most widely studied variety, 'Hayward' had the minimum FDF of 5.98 N when the FSA was 60°. Mu et al. (2020) measured its FDF at five different FSAs and reported the minimum FDF of 4.91 N at a stem angle of 120°. However, since the stem fixture is a fixed point, its measurement range is limited without FSA less than 120°. There is no fixture designed to fit kiwifruit, and relying solely on friction to fix kiwifruit can lead to inaccurate measurements. In this study, a stem fixture up to 150 mm was designed to enable a wide range of FSA measurements. A special fruit fixture allows the kiwifruit to produce less sliding due to friction during the stretching process. Fu et al. (2015) measured its FDF at three different FSAs, confirming that FSA was 1.3 to 1.7 N between 90° to 60°. However, the sliding between the flat fixture and the kiwifruit results in small measurement results. Too few angles measured can lead to the inability to obtain a complete kiwifruit separation force curve, making it difficult to find the optimal FSA.

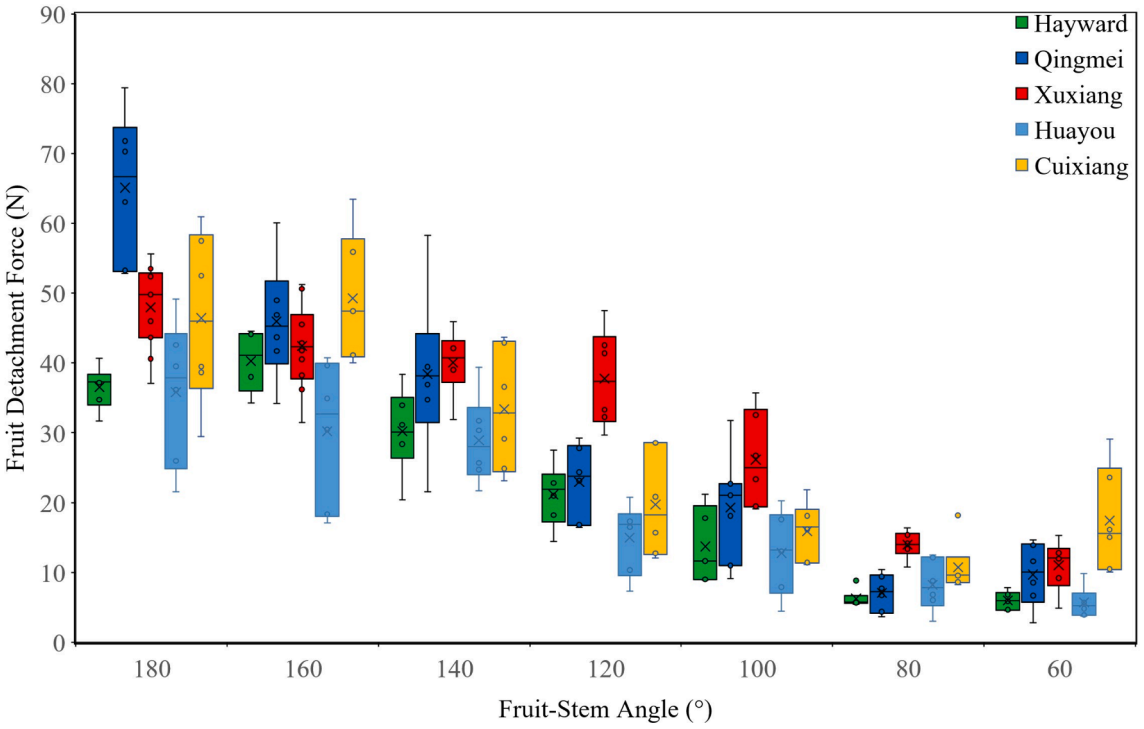


Fig. 7. Fruit detachment forces (FDFs) with the different Fruit-stem angles (FSAs) for multiple varieties kiwifruit.

Table 2
The *p*-value for the *t*-test between the FDF of the five kiwifruit varieties.

p-value	Hayward	Qinmei	Xuxiang	Cuixiang	Huayou
Hayward	1.0000	0.0580	0.0032	0.0961	0.3920
Qinmei	0.0580	1.0000	0.6976	0.5790	0.0108
Xuxiang	0.0032	0.6976	1.0000	0.2562	0.0002
Cuixiang	0.0961	0.5790	0.2562	1.0000	0.0143
Huayou	0.3920	0.0108	0.0002	0.0143	1.0000

3.3. FDF with the different FSA for multiple varieties kiwifruit

FDFs of the five varieties generally decreased with the FSA, which all decreased by more than 70% at the FSA of 60° compared to the FSA of 180°. As shown in Fig. 7, the FDF decreased from 46.36 ± 11.85 N when the FSA was 180° to 9.96 ± 4.76 N when the FSA was 60°. 'Xuxiang', which had the least decrease in the FDF with the FSA, had a 76.98% decrease in the FDF when the FSA decreased from 180° to 60°, indicating that rotation-stretch pattern is more labor-saving in fruit picking. Similar results have been found for other fruits (Li et al., 2016; Wang et al., 2021). For instance, the apple fruit detachment force required using a purely pulling motion is at least twice as when using bend-and-pull picking with a bending angle of 45° (Torregrosa et al., 2014). When a robot is picking fruit in a kiwifruit orchard, the end-effector wraps the fruit and rotates to the FSA corresponding to the minimum FDF before pulling the fruit down.

Table 3
Time needed for kiwifruit and stem detachment under different FSA.

FSA	180°	160°	140°	120°	100°	80°	60°
Time (s)	0.51 ± 0.13^{d}	0.77 ± 0.08 ^{cd}	1.25 ± 0.25^{ab}	1.14 ± 0.32^{bc}	1.34 ± 0.56^{ab}	1.43 ± 0.47^{ab}	1.65 ± 0.27^{a}

Note: Data are expressed as the mean ± standard deviation (n = 6). Different superscript letters (namely a, b, c, d) in the same row indicate significant difference (p less than 0.05) according to MANOVA (Multivariate analysis of variance) test.

FSAs corresponding to the minimum FDF of both 'Qinmei' and 'Cuixiang' were 80°, while those of other three varieties were 60°. When the FSA was 60°, 'Hayward', 'Xuxiang' and 'Huayou' had the minimum FDF with FDFs of 5.98 N, 11.04 N and 5.70 N, respectively. When the FSA was 80° instead of 60°, 'Qinmei' and 'Cuixiang' had the minimum FDF with FDFs of 7.06 N and 10.75 N, respectively. Most of the relevant studies were conducted to investigate the minimum FDF of a single variety of kiwifruit. Chen et al. (2012) reported the FDF of 7.46 N at the FSA of 90° when fruit was successfully picked in the 'Hayward' kiwifruit orchard. The fruit picking robot designed by Williams et al. (2019) was tested in three commercial orchards with only a single kiwifruit variety 'Hayward'. It is difficult to ensure good picking effect and efficiency for other varieties of kiwifruit. However, the determination of the FDF of a single variety is not suitable for the design of a robot that enables fruit picking of multiple varieties kiwifruit. Based on *t*-test analysis, there were significant differences in the FDF between kiwifruit varieties, as shown in Table 2. The FDF of 'Huayou' was significantly different from the three kiwifruit varieties (p-values for 'Qinmei', 'Xuxiang', 'Cuixiang' were found to be 0.0108, 0.0002 and 0.0143, respectively). The FDF of 'Xuxiang' was significantly different from 'Hayward', although they are similar looking kiwifruit varieties (the p-value was 0.0032). Therefore, FDFs for additional kiwifruit varieties will need to be measured in the future to help design robots capable of picking multiple varieties kiwifruit.

Variance of FDF, which represents the variability of FDF under the same FSA, generally decreased with the FSA. The variance of FDF decreased from a maximum of 72.55 N when the FSA was 180° to a minimum of 7.95 N when the FSA was 80°. However, when the FSA was 60°, the variance of the FDF was greater as compared to FSA of 80°, especially for 'Xuxiang', 'Cuixiang', and 'Huayou'. These results showed that too small or too large FSA causes an unstable FDF, which may result in unstable picking performance of the end-effector.

Interestingly, for 'Hayward' and 'Cuixiang', the FDF at the FSA of 180° was smaller than that at the FSA of 160°. When the FSA was 180°,



Fig. 8. Broken stem of 'Xuxiang' kiwifruit when the FSA was 180°.

'Qinmei', 'Xuxiang', and 'Huayou' had the maximum FDFs of 65.10 N, 47.96 N and 35.81 N, respectively. When the FSA was 160° instead of 180°, 'Hayward' and 'Cuixiang' had the maximum FDFs of 40.27 N and 49.24 N, respectively. These results show that if the FSA is limited to 180° or 160° in the orchard environment, it is more reasonable to set the FSA at 180° when fruit picking for 'Hayward' or 'Cuixiang'.

The time of stem and fruit separation under different FSAs was recorded, which indicated that the time of stem and fruit separation increased with decreasing FSA. The separation time increased from 0.51 s with FSA of 180° to 1.65 s with FSA of 60°, as shown in Table 3. The stem is usually bent when the FSA is small and first it need straightened during stem and fruit separation, which results in longer time of stem and fruit separation. Since only the effect of the FSA on the FDF was studied, there were differences in the degree of bending of stems under the same FSA, which resulted in a standard deviation of more than 40% of the mean when the FSA was 80°. Therefore, the separation time between fruit and stem in this study is difficult to be used as a basis for improving the efficiency of picking robots. However, faster robot running speed often means higher picking efficiency, which requires smaller FDF to ensure smooth picking. The FSA needs to be set smaller to ensure a smaller FDF, which keeps the vibration caused by the picking action low after increasing the operating speed of the end-effector. It could reduce the chance of damaging the fruit or getting entangled with branches.

3.4. Stem breakage of 'Xuxiang' kiwifruit

It was worth noting that, unlike other four varieties, stem breakage occurred when the FDF of 'Xuxiang' was measured at the FSA of 180° or 160°. For 'Xuxiang', the stem breakage occurred in five fruit when the FSA was 180°, and in three fruit when the FSA was 160°, as shown in Fig. 8. The stem breakage no longer occurred when the FSA was less than or equal to 140°. Stems of fruits are usually not kept after picking because of the increased risk of scratching other fruit (Villibor et al., 2019; Williams et al., 2019). Picking robots are not suitable for adding stem detection and removal components due to stability and cost requirement (Bu et al., 2020). Therefore, the FSA of 'Xuxiang' needs to be less than 160° to reduce the risk of stem breakage.

A possible cause of the stem breakage of 'Xuxiang' was the special structure at the connection between the fruit and stem. A raised wooden ring structure encloses the connection between the 'Xuxiang' fruit and stem, as shown in Fig. 9, which is different from other varieties. More stable connection caused the stem breakage of 'Xuxiang' before fruit and stem separation.

4. Conclusions

The FDF of five kiwifruit varieties was determined at seven FSA by designing a special fixture, which was installed on a texture analyzer to form an experimental platform. FDFs of five varieties generally decreased with the FSA, which corresponded to the minimum FDF of both 'Qinmei' and 'Cuixiang' being 80°, while those of other three varieties were 60°. The FDF at the FSA of 180° was smaller than that at the FSA of 160° for 'Hayward' and 'Cuixiang'. Additionally, the stem breakage occurred when the FDF of 'Xuxiang' was measured at the FSA of 180° or 160°, which is not allowed because of the increased risk of scratching other fruits.

The research work of this study has a certain significance for designing universal robotic picking end-effector, but it still needs to be further investigated in the future. For instance, research could start by focusing on the detection of multiple varieties of kiwifruit. Subsequently, picking strategy for multiple varieties of kiwifruit would enable the robot to automatically adjust fruit-stem angles (FSA) based on the variety of fruit. For the separation test between fruit and stem, the existing motion between the stem and fruit occurs within the same two-dimensional plane, which makes it difficult to cover all the situations of a real fruit picking scenario. Subsequent efforts could involve enhancing the platform for FDF with different FSAs to enable the mutual movement of stems and fruits in a 3D space.



Fig. 9. Connection point between fruit and stem of the five kiwifruit varieties. The red circle marks the raised wooden ring structure. (For interpretation of the references to colour in this figure legend, the reader is referred to the web version of this article.)

CRediT authorship contribution statement

Wentai Fang: Data curation, Investigation, Writing – original draft. **Zhenchao Wu:** Conceptualization, Methodology, Writing – review & editing. **Weiwu Li:** Data curation, Investigation. **Xiaoming Sun:** Conceptualization, Investigation, Writing – review & editing. **Wulan Mao:** Methodology, Investigation, Writing – review & editing. **Rui Li:** Methodology, Supervision, Writing – review & editing. **Yaqoob Majeed:** Conceptualization, Methodology, Writing – review & editing. **Longsheng Fu:** Conceptualization, Data curation, Methodology, Supervision, Writing – review & editing.

Declaration of Competing Interest

The authors declare that they have no known competing financial interests or personal relationships that could have appeared to influence the work reported in this paper.

Data availability

Data will be made available on request.

Acknowledgements

This work was supported by the National Natural Science Foundation of China (32371999); Key R&D Program of Zhejiang (2022C02055); Science and Technology Promotion Program of Northwest A&F University (TGZX2021-29); National Foreign Expert Project, Ministry of Science and Technology, China (DL2022172003L, QN2022172006L).

References

Au, C.K., Barnett, J., Lim, S.H., Duke, M., 2020. Workspace analysis of cartesian robot system for kiwifruit harvesting. Ind. Robot. 47 (4), 503–510. https://doi.org/10.1108/IR-12-2019-0255.

Au, C.K., Redstall, M., Duke, M., Kuang, Y.C., Lim, S.H., 2022. Obtaining the effective gripper dimensions for a kiwifruit harvesting robot using kinematic calibration procedures. Ind. Robot. 49 (5), 865–876. https://doi.org/10.1108/IR-09-2021-0198.

Bechar, A., Vigneault, C., 2016. Agricultural robots for field operations: Concepts and components. Biosyst. Eng. 149, 94–111. https://doi.org/10.1016/j.biosystemseng.2016.06.014.

Bu, L., Chen, C., Hu, G., Sugirbay, A., Chen, J., 2020. Technological development of robotic apple harvesters: A review. INMATEH - Agric. Eng. 61 (2), 151–164. https://doi.org/10.35633/inmateh-61-17.

Bu, L., Chen, C., Hu, G., Zhou, J., Sugirbay, A., Chen, J., 2021. Investigating the dynamic behavior of an apple branch-stem-fruit model using experimental and simulation analysis. Comput. Electron. Agric. 186, 106224. https://doi.org/10.1016/j.compag.2021.106224.

Chen, J., Wang, H., Jiang, H., Gao, H., Lei, W., Dang, G., 2012. Design of end-effector for kiwifruit harvesting robot. Trans. Chin. Soc. Agric. Mach. 43 (10), 151–154. https://doi.org/10.6041/j.issn.1000-1298.2012.10.027.

Feng, J., Liu, G., Si, Y., Wang, S., Zhou, W., 2013. Construction of laser vision system for apple harvesting robot. Trans. Chin. Soc. Agric. Eng. 29 (25), 32–37. https://doi.org/10.3969/j.issn.1002-6819.2013.z1.005.

Fu, L., Zhang, F., Yoshinori, G., Li, Z., Wang, B., Cui, Y., 2015. Development and experiment of end-effector for kiwifruit harvesting robot. Trans. Chin. Soc. Agric. Mach. 46 (3), 1–8. https://doi.org/10.6041/j.issn.1000-1298.2015.03.001.

Graham, S.S., Zong, W., Feng, J., Tang, S., 2018. Design and testing of a kiwifruit harvester end-effector. Trans. ASABE 61 (1), 45–51. https://doi.org/10.13031/trans.12361.

Guo, W., Wang, K., Liu, Z., Zhang, Y., Xie, D., Zhu, Z., 2020. Sensor-based in-situ detector for distinguishing between forchlorfenuron treated and untreated kiwifruit at multi-wavelengths. Biosyst. Eng. 190, 97–106. https://doi.org/10.1016/j.biosystemseng.2019.11.019.

He, L., Fu, H., Karkee, M., Zhang, Q., 2017. Effect of fruit location on apple detachment with mechanical shaking. Biosyst. Eng. 157, 63–71. https://doi.org/10.1016/j.biosystemseng.2017.02.009.

Jiang, W., Quan, L., Wei, G., Change, C., Geng, T., 2023. A conceptual evaluation of a weed control method with post-damage application of herbicides: A composite intelligent intra-row weeding robot. Soil. Till. Res. 234, 105837. https://doi.org/10.1016/j.still.2023.105837.

Jones, M.H., Bell, J., Dredge, D., Seabright, M., Scarfe, A., Duke, M., MacDonald, B., 2019. Design and testing of a heavy-duty platform for autonomous navigation in kiwifruit orchards. Biosyst. Eng. 187, 129–146. https://doi.org/10.1016/j.biosystemseng.2019.08.019.

Li, J., Karkee, M., Zhang, Q., Xiao, K., Feng, T., 2016. Characterizing apple picking patterns for robotic harvesting. Comput. Electron. Agric. 127, 633–640. https://doi.org/10.1016/j.compag.2016.07.024.

Liu, T., Luo, G., Ehsani, R., Toudeshki, A., Zou, X., Wang, H., 2018. Simulation study on the effects of tine-shaking frequency and penetrating depth on fruit detachment for citrus canopy-shaker harvesting. Comput. Electron. Agric. 148, 54–62. https://doi.org/10.1016/j.compag.2018.03.004.

Mohammadi, A., Rafiee, S., Mohtasebi, S.S., Rafiee, H., 2010. Energy inputs - yield relationship and cost analysis of kiwifruit production in Iran. Renew. Energy 35 (5), 1071–1075. https://doi.org/10.1016/j.renene.2009.09.004.

Mu, L., Liu, H., Cui, Y., Fu, L., Gejima, Y., 2018. Mechanized technologies for scaffolding cultivation in the kiwifruit industry: A review. Inf. Process. Agric. 5 (4), 401–410. https://doi.org/10.1016/j.inpa.2018.07.005.

Mu, L., Cui, G., Liu, Y., Cui, Y., Fu, L., Gejima, Y., 2020. Design and simulation of an integrated end-effector for picking kiwifruit by robot. Inf. Process. Agric. 7 (1), 58–71. https://doi.org/10.1016/j.inpa.2019.05.004.

Parameswarakumar, M., Gupta, C.P., 1991. Design parameters for vibratory mango harvesting system. Trans. ASABE 34 (1), 14–20. https://doi.org/10.13031/2013.31616.

Perini, M.A., Sin, I.N., Martinez, G.A., Civello, P.M., 2017. Measurement of expansin activity and plant cell wall creep by using a commercial texture analyzer. Electron. J. Biotechnol. 26, 12–19. https://doi.org/10.1016/j.ejbt.2016.12.003.

Sun, Y., Liu, X., Niu, C., Sun, X., Guo, Z., Qiao, Y., Liu, X., Wang, X., 2013. Relativity analysis between characteristic parameters of apricot's ripeness and its fruit removal force. Trans. Chin. Soc. Agric. Eng. 29 (23), 181–190. https://doi.org/10.3969/j.issn.1002.

Tekgüler, A., Yildiz, T., Sauk, H., 2015. Determination of spring rigidity and fruit detachment force in yomra variety hazelnut trees. AMA, Agric. Mech. Asia Afr. Lat. A. 46 (2), 13–16.

Torregrosa, A., Albert, F., Aleixos, N., Ortiz, C., Blasco, J., 2014. Analysis of the detachment of citrus fruits by vibration using artificial vision. Biosyst. Eng. 119, 1–12. https://doi.org/10.1016/j.biosystemseng.2013.12.010.

Villibor, G.P., Santos, F.L., de Queiroz, D.M., Khoury Junior, J.K., de Pinto, F., A. de C., 2019. Dynamic behavior of coffee fruit-stem system using modeling of flexible bodies. Comput. Electron. Agric. 166, 105009. https://doi.org/10.1016/j.compag.2019.105009.

Wang, D., Ding, C., Feng, Z., Cui, D., 2020. A low-cost handheld apparatus for inspection of peach firmness by sensing fruit resistance. Comput. Electron. Agric. 174, 105463. https://doi.org/10.1016/j.compag.2020.105463.

Wang, J., Li, B., Li, Z., Zubrycki, I., Granosik, G., 2021. Grasping behavior of the human hand during tomato picking. Comput. Electron. Agric. 180, 105901. https://doi.org/10.1016/j.compag.2020.105901.

Wang, W., Lu, H., Mo, C., Yang, Z., Hohimer, C.J., Qiu, G., 2017. Experiments on the mechanical harvesting of litchi and its effects on litchi storage. Trans. ASABE 60 (5), 1529–1535. https://doi.org/10.13031/trans.12185.

Williams, H.A.M., Jones, M.H., Nejati, M., Seabright, M.J., Bell, J., Penhall, N.D., Barnett, J.J., Duke, M.D., Scarfe, A.J., Ahn, H.S., Lim, J.Y., MacDonald, B.A., 2019. Robotic kiwifruit harvesting using machine vision, convolutional neural networks, and robotic arms. Biosyst. Eng. 181, 140–156. https://doi.org/10.1016/j.biosystemseng.2019.03.007.

Wu, Z., Li, G., Yang, R., Fu, L., Li, R., Wang, S., 2022. Coefficient of restitution of kiwifruit without external interference. J. Food Eng. 327, 111060. https://doi.org/10.1016/j.jfoodeng.2022.111060.

Yang, Z., Li, J., Zhang, L., Li, S., Jiwang; H., & Huang, X., 2021. Relativity analysis between characteristic parameters of off-season Longan abscission and its fruit removal force. Chin. J. Trop. Crop. 42 (10), 2986–2992. https://doi.org/10.3969/j.issn.1000-2561.2021.10.032.

Zhang, F., Li, Z., Wang, B., Fu, L., Cui, Y., 2014. Study on kiwifruit physical parameters and damage factors. J. Agric. Mech. Res. 36 (11), 141–145. https://doi.org/10.13427/j.cnki.njyi.2014.11.034.

Zhang, H., Zhao, Q., Lan, T., Geng, T., Gao, C., Yuan, Q., Zhang, Q., Xu, P., Sun, X., Liu, X., Ma, T., 2020. Comparative analysis of physicochemical characteristics, nutritional and functional components and antioxidant capacity of fifteen kiwifruit (actinidia) cultivars—Comparative analysis of fifteen kiwifruit (actinidia) cultivars. Foods 9 (9), 1267. https://doi.org/10.3390/foods9091267.

Zhou, Y., Guo, W., Ji, T., Du, R., 2023. Low-cost and handheld detector on soluble solids content and firmness of kiwifruit. Infrared Phys. Technol. 131, 104641. https://doi.org/10.1016/j.infrared.2023.104641.